8818 *Biochemistry* **2010,** *49,* 8818–8830
DOI: 10.1021/bi100557v

BIOCHEMISTRY
including biophysical chemistry & molecular biology
Article

Activation of DNA Cleavage by Oligomerization of DNA-Bound SgrAI†

Chad K. Park,‡ Amanda P. Stiteler,‡ Santosh Shah,‡ M. Imran Ghare,‡ Jurate Bitinaite,§ and Nancy C. Horton*,‡

‡*Department of Chemistry and Biochemistry, University of Arizona, Tucson, Arizona 85721, and*
§*New England Biolabs Inc., Ipswich, Massachusetts 01938-2723*

Received April 12, 2010; Revised Manuscript Received September 10, 2010

ABSTRACT: SgrAI is a type II restriction endonuclease that cuts an unusually long recognition sequence and exhibits allosteric self-modulation of DNA activity and sequence specificity. Precleaved primary site DNA has been shown to be an allosteric effector [Hingorani-Varma, K., and Bitinaite, J. (2003) *J. Biol. Chem. 278*, 40392−40399], stimulating cleavage of both primary (CR|CCGGYG, where the vertical bar indicates a cut site, R denotes A or G, and Y denotes C or T) and secondary [CR|CCGGY(A/C/T) and CR|CCGGGG] site DNA sequences. The fact that DNA is the allosteric effector of this endonuclease suggests at least two DNA binding sites on the functional SgrAI molecule, yet crystal structures of SgrAI [Dunten, P. W., et al. (2008) *Nucleic Acids Res. 36*, 5405−5416] show only one DNA duplex bound to one dimer of SgrAI. We show that SgrAI forms species larger than dimers or tetramers [high-molecular weight species (HMWS)] in the presence of sufficient concentrations of SgrAI and its primary site DNA sequence that are dependent on the concentration of the DNA-bound SgrAI dimer. Analytical ultracentrifugation indicates that the HMWS is heterogeneous, has sedimentation coefficients of 15−20 s, and is composed of possibly 4−12 DNA-bound SgrAI dimers. SgrAI bound to secondary site DNA will not form HMWS itself but can bind to HMWS formed with primary site DNA and SgrAI. Uncleaved, as well as precleaved, primary site DNA is capable of stimulating HMWS formation. Stimulation of DNA cleavage by SgrAI, at primary as well as secondary sites, is also dependent on the concentration of primary site DNA (cleaved or uncleaved) bound SgrAI dimers. SgrAI bound to secondary site DNA does not have significant stimulatory activity. We propose that the oligomers of DNA-bound SgrAI (i.e., HMWS) are the activated, or activatable, forms of the enzyme.

Type II restriction endonucleases are bacterial enzymes thought to protect their host from phage infection, by cleaving phage DNA injected into the cell prior to replication (*1*). Sequence specific endonucleases capable of cleaving longer unique recognition sequences are highly sought for genomic work, because longer sequences occur less frequently and allow the manipulation of larger DNA fragments. Most of the type II restriction endonucleases characterized to date cleave 4−6 bp recognition sites in DNA; however, SgrAI, a type IIF restriction endonuclease from *Streptomyces griseus*, cleaves an 8 bp recognition sequence, CR|CCGGYG (*2*) (R is A or G, Y is C or T, and the vertical bar denotes the site of cleavage), known as the SgrAI cognate or primary site sequence. Interestingly, SgrAI cleaves plasmids bearing two copies of its recognition sequence faster than those bearing only a single site (*3*, *4*). In addition, plasmid assays revealed that SgrAI will also cleave the sequences CR|CCGGY(A,C,T) and CR|CCGGGG, known as secondary sites, but only substantially in plasmids containing primary site sequences (*5*). Secondary sites are distinct from star sites, in that secondary sites are cleaved appreciably under solution conditions optimal for primary sequence cleavage. In contrast, star site sequences are sequences that are cleaved appreciably only under special reaction conditions, such as high enzyme concentrations or the presence of organic solvents or Mn^{2+}, and are discriminated against under optimal enzyme conditions by 2−4 orders of magnitude (*6*). The self-activation with self-modulation of sequence specificity exhibited by SgrAI is quite unusual and has not been detected before in type II restriction endonucleases.

Type II restriction endonucleases typically bind and recognize palindromic sequences as dimers (*1*, *6*), but the unusual biochemical properties exhibited by SgrAI suggest the formation of a higher-order oligomer containing altered enzymatic properties. For example, at low enzyme concentrations, SgrAI cleaves plasmids bearing one or two sites at equal rates, but higher enzyme concentrations result in faster cleavage of the two-site plasmid (*4*, *7*). Similarly, the DNA cleavage turnover number, k_{cat}, of SgrAI with its primary sequence shows a sigmoidal dependence on SgrAI concentration, consistent with the formation of an activated oligomer at the higher enzyme concentrations (*4*, *7*). The stimulation of DNA cleavage activity must occur through three-dimensional space, as the accelerated and concerted cleavage also occurs with plasmids each bearing a single site but connected by catenation (*7*). Cleavage at primary and secondary site sequences in plasmids can also be stimulated by the addition of oligonucleotides containing the primary site sequence, intact or mimicking the cleavage products of SgrAI (*5*, *7*, *8*), indicating that DNA is the allosteric effector, and that the functional unit of stimulated SgrAI has at least two DNA binding sites. (An alternative mechanism would involve the memory of the binding of cleaved primary site after its dissociation. Such mechanisms typically require a covalent modification if oligomerization is absent.) Analytical ultracentrifugation shows that SgrAI exists as a dimer in the absence of DNA but forms both DNA-bound

†This work was supported by National Institutes of Health Grant GM066805 to N.C.H. and the Howard Hughes Medical Institute (Grant 52005889 to the University of Arizona supporting M.I.G.).

*To whom correspondence should be addressed. Telephone: (520) 626-3828. Fax: (520) 621-9288. E-mail: nhorton@u.arizona.edu.

 Published on Web 09/13/2010

dimers and high-molecular mass aggregates in the presence of a 20 bp DNA containing a primary site (*4*). The stoichiometry of this mixture of species has been determined by titration of DNA with SgrAI in analytical untracentrifuge sedimentation velocity experiments showing one dimer of SgrAI per DNA duplex (*4*). A reasonable model for the oligomerization of DNA-bound dimers (DBDs)[1], which will bring two DNA binding sites together into a single functional unit of the enzyme, is the formation of a tetramer, because the evolutionarily related enzymes NgoMIV, Cfr10I, and Bse634I form tetramers that bind to two duplexes of DNA. However, we show here that rather than tetramers, SgrAI forms larger oligomers of DBD (HMWS) containing possibly as many as 4−12 DNA-bound SgrAI dimers. The HMWS is formed with primary site DNA, which need not be cleaved. SgrAI dimers bound to secondary site DNA will not form HMWS unless sufficient concentrations of SgrAI dimers bound to primary site are also present. Because the stimulation of the single-turnover rate of DNA cleavage (on primary or secondary site DNA) also depends on the presence of sufficient concentrations of SgrAI bound to primary site DNA, conditions where HMWS form, we conclude that the HMWS is composed of many DBD and is the activated, or activatable, form of SgrAI.

EXPERIMENTAL PROCEDURES

Protein Purification. Wild-type SgrAI was prepared as described previously (*9*). Briefly, SgrAI was expressed in *Escherichia coli* strain ER2566 in the presence of the MspI methyltransferase (New England Biolabs). The enzyme was purified using FPLC (GE Healthcare Biosciences) and the following chromatographic resins: Heparin FF Sepharose (Pharmacia), SP FF Sepharose (GE Healthcare Biosciences), Q FF Sepharose (GE Healthcare Biosciences), and then a second Heparin FF Sepharose (GE Healthcare Biosciences) chromatographic step. Finally, the SgrAI enzyme was dialyzed into storage buffer [20 mM Tris-OAc (pH 8.0), 50 mM KOAc, 0.1 mM EDTA, 1 mM DTT, and 50% glycerol], aliquoted into single-use aliquots, flash-frozen in liquid nitrogen, and stored at −80 °C.

DNA Preparation. The oligonucleotides were made synthetically and purified using C18 reverse phase HPLC (*10*). The concentration was measured spectrophotometrically, with an extinction coefficient calculated from standard values for the nucleotides (*11*), and fluorophore where appropriate. Fluorophore-labeled DNA utilized a 6-(3′,6′-dipivaloylfluoresceinyl-6-carboxamido)hexyl (FLO) group attached to the 5′-phosphate of the top strand of the precleaved 40 bp primary site containing DNA (FLO-PCP), or a 6-[4,7,2′,4′,5′,7′-hexachloro(3′,6′-dipivaloyl-fluoresceinyl)-6-carboxamido]hexyl (HEX) group attached to the 5′-phosphate of both strands (HEX-18-1) or only the top strands of the 18 bp secondary site DNA (HEX-18-2) and 40 bp primary site containing DNA (HEX-40-1), and was obtained from a commercial synthetic source (Sigma Genosys, Inc.) and contains a six-carbon spacer between the fluorophore and the 5′-phosphate. The self cDNA or equimolar quantities of cDNA were annealed by being heated to 90 °C for 10 min at a concentration of 1 mM, followed by slow cooling to 4 °C over 4−5 h in a thermocycler. Sequences of the DNA used are

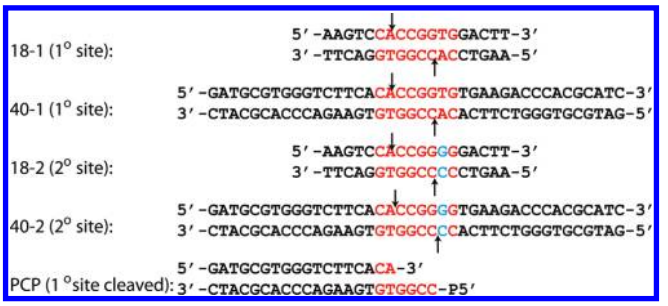

Because freezing and thawing altered the concentration of double-stranded DNA used in the assays, DNA used for stimulation of HMWS formation or in single-turnover assays was treated very carefully to minimize this problem. Such DNA samples were either reannealed immediately prior to the assay or carefully annealed, assessed for concentration, aliquoted into small amounts, flash-frozen in liquid nitrogen, stored at −20 °C (in water), and used only once after being removed from the freezer. DNA was 5′ end labeled with ^{32}P using T4 polynucleotide kinase (New England Biolabs) and [γ-^{32}P]ATP (Perkin-Elmer, Inc.), and excess ATP was removed using G-30 spin columns (Bio-Rad Laboratories, Inc.).

BINDING ASSAYS

Fluorescence Polarization Anisotropy (*FPA*). The equilibrium dissociation constant, K_D, of SgrAI−DNA complexes was measured using a fluorescence polarization anisotropy (FPA) technique (*12*). DNA oligonucleotides [1 nM in 2 mL of binding buffer, which consisted of 20 mM Tris-OAc (pH 8.0), 50 mM KOAc, 10 mM $Ca(OAc)_2$, 1 mM DTT, and 10% glycerol at 4 °C] containing a fluorophore (HEX or FLO) ligated to the 5′ end were titrated with increasing amounts of SgrAI enzyme (from 1 nM to 1 μM), and the polarization of the emitted fluorescence was monitored. Excitation occurred at 537 nm (HEX) or 492 nm (FLO) in a PC1 (ISS) fluorimeter with T format, automatic polarizers and temperature control. The emitted intensities were measured using a 50.8 mm diameter 570 nm cuton filter with a 580−2750 nm transmittance range (ThermoOriel Inc., catalog no. 59510) and 1 mm slit widths. The polarization of the emitted light as a function of added enzyme was fit to a 1:1 binding model using Kaleidagraph and the following equation (*12*):

$$A = A_{min} + (A_{max} - A_{min})\{P_T + O_T + K_D - [(P_T+O_T+K_D)^2 - (4P_TO_T)]^{1/2}\}/(2O_T)$$

where A is the polarization at a given protein concentration, A_{max} is the predicted polarization of fully bound DNA, A_{min} is the polarization with no protein binding, P_T is the total concentration of protein, O_T is the total concentration of the DNA, and K_D is the dissociation constant to be determined.

Gel Shift. The gel shift assay (*13*) was also used to measure binding affinities of SgrAI for DNA. DNA oligonucleotides were 5′ end labeled (*14*) with ^{32}P and held constant at a concentration of 10 pM in 20 μL of binding buffer [20 mM Tris-OAc (pH 8.0), 50 mM KOAc, 10 mM $Ca(OAc)_2$, 1 mM DTT, and 10% glycerol at 4 °C]. Separate incubations were performed with the DNA and

[1]Abbreviations: DBD, DNA-bound SgrAI dimer; DTT, dithiothreitol; EDTA, ethylenediaminetetraacetic acid; FLO, fluorescein moiety; FPA, fluorescence polarization anisotropy; HEX, hexachlorofluorescein moiety; HMWS, high-molecular weight species; OAc, acetate; PAGE, polyacrylamide gel electrophoresis; PC, precleaved primary site DNA without the 5′ end at the cleavage site phosphorylated; PCP, precleaved primary site DNA with the 5′ end at the cleavage site phosphorylated; rmsd, root-mean-square deviation.

varied concentrations of SgrAI enzyme (from 10 pM to 1 μM). These concentrations were chosen carefully to give a well-defined binding curve. Native PAGE (8 to 10% 19:1 or 29:1 acrylamide: bisacrylamide, 89 mM Tris, 89 mM boric acid, and 10 mM Ca^{2+}) was used to separate the bound and unbound DNA, as the DNA bound to SgrAI will have a reduced electrophoretic mobility. Care was taken to prevent heating of the gel, by conducting the experiments at 4 °C at a low voltage (190 V). The electrophoresis buffer (89 mM Tris, 89 mM boric acid, and 10 mM Ca^{2+}) was recirculated during electrophoresis. Gels were loaded while undergoing electrophoresis at 300 V, and the voltage returned to 190 V 5 min after the last sample had been loaded. Gels were then subjected to electrophoresis for an additional 2 h at 4 °C. Autoradiography of gels was performed without drying with a phosphor image plate exposed at 4 °C for 12−17 h. Densitometry of phosphor image plates was performed with a Typhoon Scanner (GE Healthcare Life Sciences), and integration using ImageQuant (GE Healthcare Life Sciences) or ImageJ (*15*). The equilibrium dissociation constant, K_D, was determined as described above for the FPA measurements, using normalized values of the amount of shifted DNA for each concentration of SgrAI.

Single-Turnover DNA Cleavage Assays. Single-turnover measurements of DNA cleavage were performed using chemical rapid quench techniques and ^{32}P 5′ end labeled oligonucleotide substrates (typically 1 nM), under conditions of excess enzyme (1 μM), with and without the addition of unlabeled DNA. All reactions were performed at 37 °C in 20 mM Tris-OAc (pH 8.0), 50 mM KOAc, 10 mM $Mg(OAc)_2$, and 1 mM DTT. For sampling by hand, 5 μL aliquots were withdrawn at specific time intervals after the enzyme had been mixed with labeled DNA (total reaction volume of 100 μL), quenched by addition to 5 μL of quench (80% formamide and 50 mM EDTA), and electrophoresed on 20% denaturing polyacrylamide (19:1 acrylamide: bisacrylamide, 4 M urea, 89 mM Tris, 89 mM boric acid, and 2 mM EDTA) gels. Autoradiography of gels was performed without drying with a phosphor image plate exposed at 4 °C for 12−17 h. Densitometry of phosphor image plates was performed with a Typhoon Scanner (GE Healthcare Life Sciences), and integration using ImageQuant (GE Healthcare Life Sciences) or ImageJ (*15*). The percent of product formed as a function of time was determined by integrating both cleaved and uncleaved DNA bands. The single-turnover DNA cleavage rate constant was determined from the data using a single-exponential function:

$$\% \text{ product} = C_1 + C_2(1 - e^{-kt})$$

where C_1 is a constant fitting the baseline, C_2 is the total percent of DNA predicted to be cleaved by SgrAI, k is the rate constant, and t is the length of incubation in minutes. To achieve time points faster than 10 s, a RQF-3 rapid quench flow instrument (KinTek Inc.) was used according to a method modified from that of the instrument manual. Because dilution of the samples was a concern using samples in the sample loops, the enzyme and DNA solutions were instead placed in drive syringes A and B, respectively. Quench solution was used in the C syringe. For the reactions, loop 3 (40 μL) was used in a two-step push. Each step was conducted at 500 rpm (7475 μL/s) to ensure good mixing (Re = 11900). Each step pushed 64 μL from each syringe (128 μL total). The reaction time was set by the time between the two steps and was controlled by the instruments' computer. The step size was chosen such that the sample loop would be completely filled in one step and ejected in the second step.

Native Gel Analysis of HMWS Formation. Formation of HMWS was monitored using native PAGE and the method described above for gel shift measurements with the following modifications. The acrylamide composition was 8% 29:1 acrylamide:bisacrylamide, and samples were prepared with 1 μM SgrAI, 1 nM ^{32}P-labeled DNA, and varied concentrations of unlabeled DNA in binding buffer [20 mM Tris-OAc (pH 8.0), 50 mM KOAc, 10 mM $Ca(OAc)_2$, 1 nM DTT, and 10% glycerol] in a volume of 20 μL. The effect of increased ionic strength was tested using buffers with varied concentrations (0−300 mM) of KOAc or NaCl in place of the 50 mM KOAc. Prepared samples were incubated for 30 min at 4 °C prior to electrophoresis. Integrated band intensities were normalized using the sum of the DNA-bound species (DBD and HMWS) to determine the percent HMWS.

Sedimentation Velocity. Sedimentation velocity experiments were performed in a Beckman Coulter XL-I instrument equipped with a monochromator and interference scanning optics (632 nm) using a Ti-50 rotor. Two sector sedimentation velocity cells were loaded with approximately 400 μL of sample containing 3 μM fluorophore-labeled DNA with or without 6 μM SgrAI in one sector and 425 μL of buffer in the other. The buffers used in the measurements contained 20 mM Tris-OAc (pH 8.0), 1 mM DTT, either 50 mM KOAc or 150 mM NaCl, and either 10 mM $Ca(OAc)_2$ or 10 mM $Mg(OAc)_2$. After sealing the cell and loading, balancing, and installing the rotor, we allowed the system to equilibrate for at least 1 h after reaching the target temperature (4 or 37 °C). The sample was spun at 40000 rpm (115000*g*), and absorbance scans were taken at 495 nm (FLO-PCP) or 537 nm (HEX-18-2) continuously, with a 0.003 cm step stize, until the last of the boundaries had moved to the bottom of the solution column (at least 12−17 h). Data from the scans were fit to a sedimentation coefficient distribution, $c(s)$, using SEDFIT (*16*). The SgrAI dimer partial specific volume was calculated using SEDNTERP (*17*). Only a single partial specific volume can be used in the data analysis with SEDFIT, and that of the 1:1 SgrAI dimer−DNA duplex was used [calculated using a weighted, by their respective molecular weights, average of the partial specific volumes of the protein (0.74 mL/g) and DNA (0.55 mL/g)]. This same partial specific volume was also used in the analysis of data from samples containing only DNA, to allow for the assignment of the peaks corresponding to the unbound DNA in the SgrAI/DNA mixtures. Viscosities and densities were calculated using SEDNTERP (*17*). Because of limited component selection, SEDNTERP calculations utilized the parameters of potassium sulfate, magnesium sulfate, and calcium chloride for potassium acetate, magnesium acetate, and calcium acetate of the buffers, respectively. Calculated values for buffers similar to those used in these studies have been found to be within 1% error of the values measured experimentally using a Mettler-Toledo five-place densitometer and Canon-Fenske viscometer.

Sedimentation Equilibrium. Sedimentation equilibrium experiments were performed as described above for sedimentation velocity with the following modifications. Samples (110 μL) containing varied concentrations of SgrAI (3−12 μM) and fluorophore-labeled DNA (1.5−6 μM) were loaded into three chambers of a six-chamber centerpiece, with buffer occupying the remaining three. The system was allowed to equilibrate for at least 1 h after reaching the target temperature (4 or 37 °C). Samples were then subjected to centrifugal speeds from 4000 to 18000 rpm for a period of 72−96 h. High-resolution scans were taken at 492 nm (FLO-PCP) or 537 nm (HEX-18-2) every 4 h,

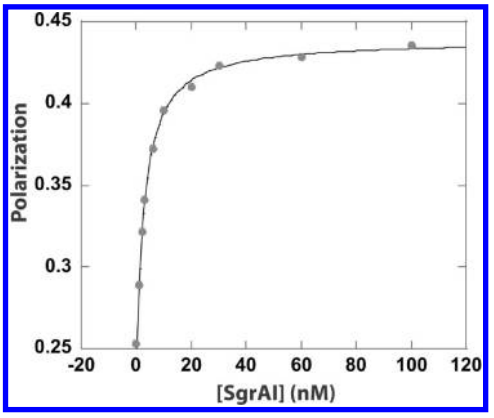

FIGURE 1: Fluorescence polarization anisotropy (FPA) measurement (gray filled circles) of SgrAI binding to FLO-labeled PCP in buffer 3 (Table 1 legend) at 4 °C. The line shows a fit (see Experimental Procedures) to a 1:1 binding model giving a K_D of 10.8 ± 0.5 nM with an R of 0.99965.

Table 1: Equilibrium Dissociation Constants for 1 μM Wild-Type SgrAI Dimer and DNA Sequences at 4 °C

DNA[a]	buffer[b]	K_D[c] (nM), FPA	K_D[c] (nM), gel shift
18-1	1	2.5 ± 0.9	0.6 ± 0.2
18-2	1	1.5 ± 0.2	2.6 ± 1.2
40-1	1	0.9 ± 0.2	0.057 ± 0.009
PCP	1	6 ± 2	not determined
PC	1	5 ± 1	not determined
PCP	2	3 ± 1	not determined
PCP	3	14 ± 4	not determined

[a]FPA utilized HEX-labeled 18-1, 40-1, and 18-2, FLO-labeled PCP, and PC. [b]Buffer 1 consisted of 20 mM Tris-acetate (pH 8.0), 50 mM KOAc, 10 mM $Ca(OAc)_2$, 1 mM DTT, and 10% glycerol. Buffer 2 consisted of 20 mM Tris-acetate (pH 8.0), 50 mM KOAc, 10 mM $Ca(OAc)_2$, and 1 mM DTT. Buffer 3 consisted of 20 mM Tris-acetate (pH 8.0), 50 mM KOAc, 10 mM $Mg(OAc)_2$, and 1 mM DTT. [c]Equilibrium dissociation constants, K_D, given as the average of at least three different measurements ± the standard deviation, and assuming 1:1 binding.

with a step size of 0.001 cm. Equilibrium was established when a reasonable (< 0.07) and constant rmsd was found between sequential scans. The data were analyzed using global fitting in SEDFIT (*16*) with a single species. Density and partial specific volumes were determined as described above.

RESULTS

DNA Binding Assays. The equilibrium dissociation binding constants (K_D) of SgrAI and various DNA oligonucleotide constructs containing intact primary site DNA (18-1 and 40-1), secondary site DNA (18-2 and 40-2), or precleaved 40 bp primary site containing DNA (PCP or PC) were measured using a fluorescence polarization assay [FPA (Figure 1)] or a gel shift assay (Table 1). The measurements were taken at 4 °C in 20 mM Tris-OAc (pH 8.0), 50 mM KOAc, 10 mM $Ca(OAc)_2$, 1 mM DTT, and 10% glycerol (unless otherwise noted) and are presented as the average of at least three independent measurements ± the standard deviation. Ca^{2+} was used as a substitute for Mg^{2+}, as numerous studies show that this substitution retains binding specificity without conferring DNA cleavage activity (*12*, *18*−*21*). All of the binding isotherms fit very well to a model for 1:1 binding (see Experimental Procedures). Differences in K_D values measured by the two methods can be explained by the difficulty in measuring K_D values smaller than 1 nM using FPA, because DNA concentrations of < 1 nM are too weak to detect using this method. In such cases, the gel shift measurements (using 10 pM ^{32}P-labeled DNA) are likely to be more reliable. The results show that SgrAI binds to primary site-containing DNA with a K_D of 0.6 ± 0.2 nM (by gel shift) when embedded in an 18 bp DNA (18-1), and tighter [K_D = 0.057 ± 0.009 nM (by gel shift)] when embedded in a 40 bp DNA (40-1). The measurements show that a primary site with more flanking DNA binds tighter to SgrAI. The values are comparable to previously published measurements; for example, Daniels et al. (*4*) measured a K_D for SgrAI and a 20 bp duplex containing a primary site of 1.8 ± 0.4 nM, comparable to our measurement with 18 bp primary site containing DNA (18-1) (0.6 ± 0.2 nM). Hingorani-Varma and Bitinaite (*8*) measured values of 0.016 ± 0.002 nM for the primary site in an 80 bp duplex and 0.019 ± 0.002 nM when in a 30 bp duplex, only ~2-fold tighter than our measurement for the 40 bp primary site-containing DNA (40-1) (0.057 ± 0.009 nM). Differences in the measured K_D values could be due to a slightly different buffer composition and the temperature of the measurements (room temperature vs 4 °C).

The affinity for secondary site DNA (in an 18 bp DNA) is surprisingly strong, with a K_D of 1.5 ± 0.2 (by FPA) or 2.6 ± 1.2 nM (by gel shift). Therefore, the lower activity of SgrAI on secondary site DNA does not appear to derive from weakened binding. Our measured affinity of SgrAI for secondary site DNA is comparable to that measured previously for a different secondary site, CACCGGCT, embedded in an 80 bp duplex, of 0.7 ± 0.1 nM (*8*), with the tighter binding possibly due to the longer flanking DNA sequences.

The affinity for a mimic of cleaved 40 bp primary site DNA (PCP) is also surprisingly strong (K_D = 6 ± 2 nM by FPA). This DNA has been synthesized to contain the 5′-phosphate that would be present after cleavage of a primary site by SgrAI. The construct PC is identical with PCP but without the 5′-phosphate. The binding affinity of PC for SgrAI has been measured with a K_D of 5 ± 1 nM (by FPA). Therefore, the presence of the 5′-phosphate at the cleavage site affects binding affinity very little, consistent with previously published observations that the absence of the 5′-phosphate does not affect the stimulatory activity of the precleaved primary site (*5*, *7*, *8*). Using a competition method and the gel shift assay, the affinity for a 38 bp duplex with two "SgrAI-cleaved ends" (although no 5′-phosphate on these ends) was determined to be 0.36 ± 0.04 nM (*8*), ~17-fold tighter than our measurement by FPA; however, the DNA construct contains twice as many "cleaved ends" as PCP. The cleaved end of PCP contains a single-stranded overhang that would be left after cleavage of a primary site by SgrAI, 5′-CCGG-3′, and also contains the phosphate at the 5′ end of this overhang to better mimic the naturally cleaved ends.

The affinity of SgrAI for PCP in buffer without glycerol (but with 10 mM Ca^{2+}) was measured with a K_D of 3 ± 1 nM (by FPA), indicating that the 10% glycerol of the binding buffer also has little affect on the binding affinity. Because PCP cannot be cleaved further by SgrAI, the binding affinity for this DNA could also be measured in the presence of Mg^{2+}, rather than Ca^{2+}, and was found to have a K_D of 14 ± 4 nM (by FPA). Therefore, use of Ca^{2+} in place of Mg^{2+} appears to have the effect of tightening the DNA binding affinity by ~3-fold.

Stoichiometric measurements were performed with SgrAI and the 18 bp DNA containing the primary site sequence (18-1), as well as the 18 bp DNA containing the secondary site sequence (18-2), using FPA or the gel shift method. In this method, 75−100 nM DNA is titrated with SgrAI until a break is seen

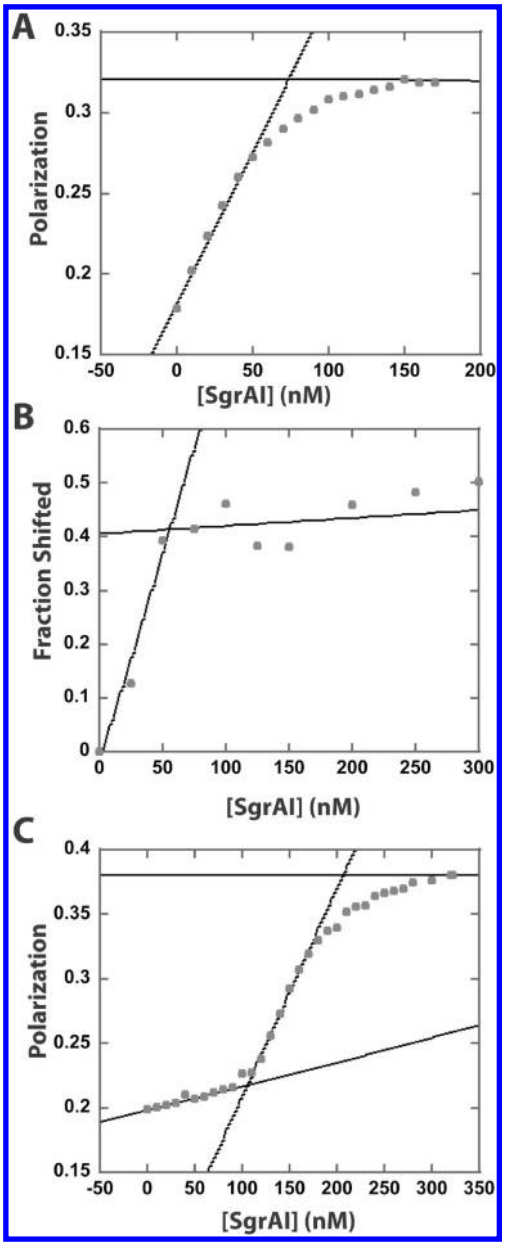

FIGURE 2: Determination of the stoichiometry of binding of SgrAI to 18-2 and 18-1. (A) Titration of 75 nM HEX-labeled 18-2 in buffer 2 (Table 1) at 4 °C. The intercept of the two lines is 69 nM SgrAI dimer, indicating a 1:1 stoichiometry of SgrAI dimer to 18-2 duplex with 92% of the activity of the SgrAI enzyme. (B) Native PAGE gel shift of 100 nM ^{32}P-labeled 18-1 (of which 40% is double-stranded). The intercept occurs at 55 nM SgrAI, suggesting 1:1 binding of 18-1 to the SgrAI dimer with 73% enzyme activity. (C) Titration of 100 nM HEX-labeled 18-1 in buffer 2 (Table 1) at 4 °C. The first intercept at 109 nM SgrAI dimer indicates a 1:1 stoichiometry of SgrAI dimer to 18-1 duplex with 92% of the activity of the SgrAI enzyme, and the second intercept at 207 nM SgrAI dimer indicates a second SgrAI dimer binds the original 1:1 complex.

(Figure 2), giving the concentration of the SgrAI dimer that fully saturates all binding sites on the DNA. The expected 1:1 binding is seen for secondary site DNA using HEX-labeled 18-2 and FPA (Figure 2A), and 18-1 using ^{32}P-labeled 18-1 and the gel shift assay (Figure 2B). However, two breaks are seen in the plot of polarization versus SgrAI concentration with HEX-labeled 18-1, one at 1:1 binding and one at 2:1 SgrAI dimers per 18-1 duplex (Figure 2C). Hence, a second dimer, binding more weakly than the first, appears to add to the SgrAI dimer−HEX-18-1 complex. The binding of additional SgrAI dimers to the 1:1 saturated

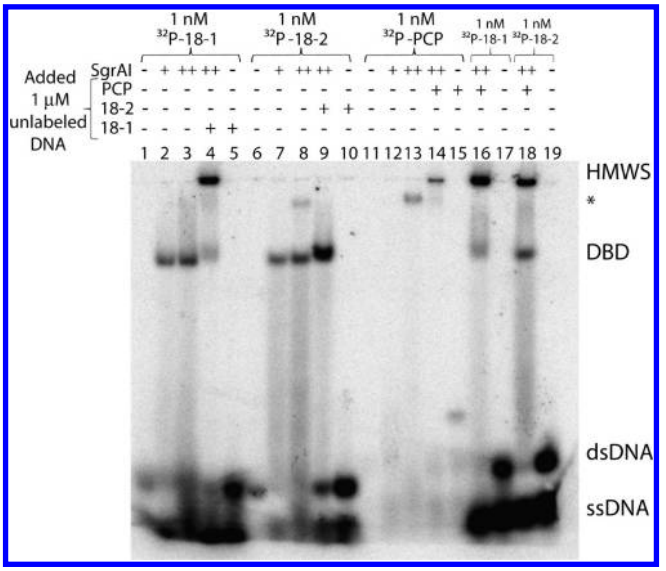

FIGURE 3: Autoradiogram of native PAGE with 1 nM ^{32}P-labeled DNA as indicated and varied additions, including 1 μM unlabeled 18-1, 18-2, or PCP DNA (+), 50 nM SgrAI dimer (+), and/or 1 μM SgrAI dimer (++). The asterisk denotes DBDs bound to one or more additional SgrAI dimers.

primary site has been seen before, also using FPA, although the second binding was not titrated to completion (*4*).

All of the binding isotherms used to measure the K_D (with 1 nM DNA) fit very well to a model for 1:1 binding without cooperativity (Figure 1), most likely indicating that the additional SgrAI dimers do not bind at the low nanomolar concentrations of the SgrAI−DNA complex. The fit to the 1:1 binding model also suggests that only a single duplex of DNA binds to one SgrAI binding site, which was surprising in the case of PCP, because two molecules of PCP are equivalent to one complete primary site DNA. Because unbound SgrAI is dimeric under the conditions of the binding measurements [as determined by analytical ultracentrifugation (*4*)], the fit to 1:1 binding without any evidence of cooperativity could mean that one molecule of PCP binds to one dimer of SgrAI. Alternatively, it could mean that two molecules of PCP bind uncooperatively to the SgrAI dimer having two independent binding sites, but this appears intuitively unlikely because the single-stranded 5′-CCGG-3′ overhangs would be expected to anneal in the enzyme binding site and therefore interact cooperatively. Still a third possibility is that SgrAI binds to one molecule of DNA, composed of two PCP molecules. Because the binding measurements were performed at 4 °C, and the T_m of the single-stranded overhangs of PCP, 5′-CCGG-3′, is calculated to be 16 °C, the binding data determined at 4 °C likely represent the binding of SgrAI to one molecule of annealed PCP, comprised of two PCP molecules.

Characterization of HMWS Using Native Gel Electrophoresis. We have determined conditions for separating DNA-bound dimers of SgrAI (DBD) from a high-molecular weight species [HMWS (Figure 3)] composed of SgrAI and DNA using native polyacrylamide gel electrophoresis at 4 °C. The binding reaction mixtures were prepared in binding buffer [20 mM Tris-OAc (pH 8.0), 50 mM KOAc, 1 mM DTT, 10 mM $Ca(OAc)_2$, and 10% glycerol] with 1 nM ^{32}P-labeled DNA and varied concentrations (typically 1 μM) of SgrAI. Additional unlabeled DNA was added in these experiments, in the range of 1−3000 nM. Using the native PAGE, we observed two shifted bands; the faster-moving band was identified as dimeric SgrAI bound to

DNA (i.e., DBD), because analytical ultracentrifugation (see below and ref *4*) has shown that only DBD is formed with secondary site DNA, and lane 9 in Figure 3, mimicking the conditions used in the analytical ultracentrifugation, shows only this species. The HMWS is so named because it runs slower than DBD; however, the exact composition of HMWS cannot be determined from the gel (see below for analytical ultracentrifugation of HMWS). Using this native gel assay, we have discovered that the formation of HMWS depends upon the concentration of DBD, as well as the sequence of bound DNA. Only DBD form with 1 nM ^{32}P-labeled uncleaved DNA and 1 μM SgrAI dimer, whether the DNA is the primary or secondary site DNA (Figure 3, lanes 2 and 3 and lanes 7 and 8); however, with primary site DNA at concentrations of 1 μM DNA (with 1 nM ^{32}P-labeled DNA and 1 μM SgrAI dimer), both DBD and HMWS are found (Figure 3, lane 4). HMWS is never formed with only secondary site DNA, regardless of the concentration of DNA or SgrAI (Figure 3, lanes 6−10) or length (18 or 40 bp, Figure 4C). However, HMWS will form with 1 nM ^{32}P-labeled secondary site DNA in the presence of 1 μM SgrAI and 1 μM unlabeled precleaved 40 bp primary site DNA (PCP) (Figure 3, lane 18). PCP binds with nanomolar affinity to SgrAI (Table 1); however, at 50 nM SgrAI and 1 nM ^{32}P-labeled PCP, the complex appears to be too labile to form a shifted band (Figure 3, lane 12). This could be due to differences in the temperature at which the two measurements were performed. Both were performed at 4 °C; however, local heating can occur in the gel during electrophoresis. PCP contains a four-nucleotide self-complementary single-stranded overhang (5′-CCGG-3′) that anneals to itself with a calculated T_m of 16 °C to form a 40 bp duplex, which may bind tighter to SgrAI than the unannealed form. In addition, a band running more slowly than the DNA-bound dimer appears at 1 μM SgrAI dimer and 1 nM ^{32}P-labeled PCP (Figure 3, lane 13), suggesting a propensity for additional SgrAI dimers to bind to the DNA-bound dimer of SgrAI (DBD) at these concentrations, which is seen with 1 μM SgrAI dimer and 1 nM 18 bp DNA containing the secondary site sequence (18-2) (Figure 3, lane 8), and 1 nM 18 bp DNA containing the primary site sequence (18-1) when analyzed by FPA (see above). At 1 μM SgrAI dimer and 1 μM PCP (of which 1 nM is ^{32}P-labeled), only HMWS is observed (Figure 3, lane 14).

The precleaved 40 bp primary site-containing DNA (PCP) induces HMWS with 1 nM ^{32}P-labeled uncleaved primary site-containing DNA (18-1; Figure 3, lane 16) and with an 18 bp secondary site-containing DNA (18-2; Figure 3, lane 18) in a concentration-dependent manner (Figure 4A,B). Side-by-side comparisons of HMWS formation on ^{32}P-labeled 18-1 (with 1 μM SgrAI) as a function of DNA concentration show that PCP, 40-1, and 18-1 induce HMWS similarly (Figure 4C). This is somewhat unexpected as one might expect that twice as much precleaved 40 bp primary site-containing DNA (PCP) as uncleaved (40-1) would be required to induce the same amount of HMWS if two PCPs bind to one dimer. This result may indicate 1:1 binding of PCP to SgrAI dimer or that SgrAI bound to PCP is better able to stimulate the HMWS.

The effect of an increased ionic strength on the stability of the high-molecular weight species (HMWS) was tested using increasing concentrations of either KOAc or NaCl in buffer containing 20 mM Tris-OAc (pH 8.0), 10 mM $Ca(OAc)_2$, 10% glycerol, and 1 mM DTT (Figure 5). The samples were electrophoresed at 4 °C as described above after incubation for 30 min at 4 °C. Lanes 1 and 2 contained samples that mark the positions of unbound DNA [lane 1, containing 1 nM ^{32}P-labeled 18 bp primary site-containing DNA (18-1) only] and DBD (DNA-bound SgrAI dimer, lane 2, containing 1 nM [^{32}P]18-1 and 1 μM SgrAI). Samples loaded into lanes 3−16 each contained 1 nM ^{32}P-labeled 18-1, 1 μM SgrAI, and 1 μM precleaved 40 bp primary site-containing DNA (PC) under the different buffer conditions, and all lanes show a clear HMWS band. The samples loaded into lanes 3 and 10 contained no added KOAc or NaCl, while lanes 4−9 contained samples incubated in buffer with concentrations of KOAc increasing from 50 to 300 mM, in 50 mM increments. Similarly, lanes 11−16 show the results from samples containing increasing concentrations of NaCl, from 50 to 300 mM. Clearly, the higher salt concentrations of the incubation buffer do not eliminate the appearance of the HMWS.

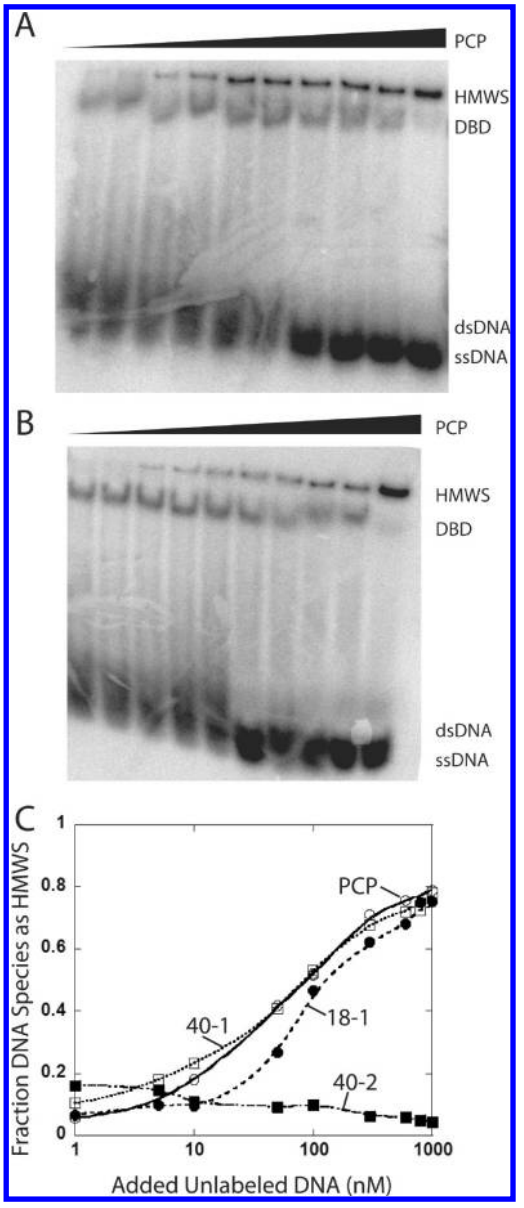

FIGURE 4: Native gel electrophoresis of 1 nM ^{32}P-labeled 18 bp DNA and 1 μM SgrAI dimer and varied concentrations of unlabeled DNA. (A) ^{32}P-labeled primary site (18-1, 1 nM) with added unlabeled PCP (10, 30, 60, 100, 200, 300, 400, 500, 600, or 1000 nM). (B) ^{32}P-labeled secondary site (18-2, 1 nM) with added unlabeled PCP (10, 30, 60, 100, 200, 300, 400, 500, 600, or 1000 nM). (C) Plot of the percent of DNA (1 nM [^{32}P]18-1)-bound species with 1 μM SgrAI found in HMWS vs concentration of added unlabeled PCP (○), 40-1 (□), 18-1 (●), or 40-2 (■).

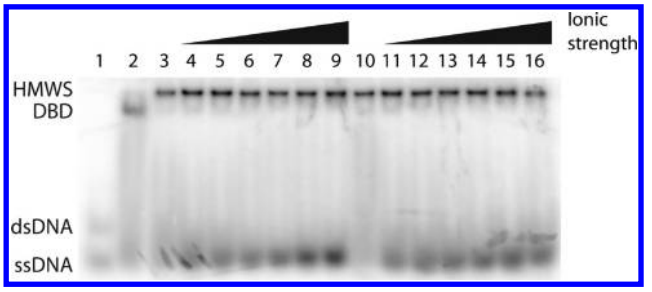

FIGURE 5: Native gel electrophoresis of samples in binding buffer containing KOAc or NaCl concentrations from 0 to 300 mM. All samples contained 1 nM [^{32}P]18-1 DNA, 1 μM SgrAI, and 1 μM PC DNA with the exception of that loaded in lane 1, which contained only [^{32}P]18-1, and lane 2, which contained [^{32}P]18-1 and SgrAI. All samples were incubated in buffer containing 20 mM Tris-OAc (pH 8.0), 10 mM $Ca(OAc)_2$, 10% glycerol, 1 mM DTT, and varied concentrations of KOAc (lanes 4−9, with 50, 100, 150, 200, 250, and 300 mM, respectively) or NaCl (lanes 11−16, with 50, 100, 150, 200, 250, and 300 mM, respectively). Samples loaded in lanes 1−3 and 10 contained no KOAc or NaCl.

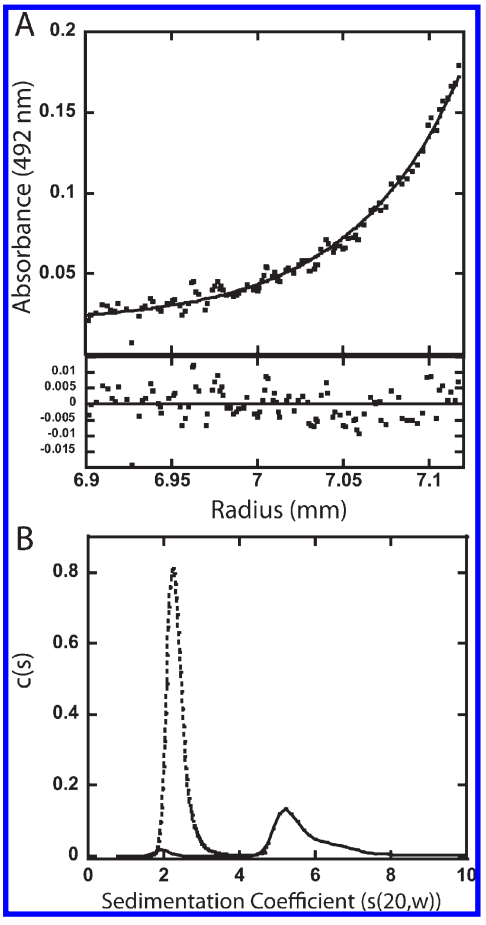

FIGURE 6: Analytical ultracentrifugation of SgrAI with secondary site-containing DNA (HEX-18-2). (A) Sedimentation equilibrium experiment with 7 μM SgrAI and 3.6 μM HEX-18-2 in 20 mM Tris-OAc (pH 8.0), 50 mM KOAc, 1 mM DTT, and 10 mM $Ca(OAc)_2$ at 4 °C and 13500 rpm. In the top panel, data are shown as filled circles and the line corresponds to a fit of a single species with a molecular mass of 90.7 kDa. The bottom panel shows residuals between the fit and data. (B) Sedimentation velocity $c(s)$ distribution of 6 μM SgrAI and 3 μM HEX-18-2 in 20 mM Tris-OAc (pH 8.0), 50 mM KOAc, 1 mM DTT, and 10 mM $Ca(OAc)_2$ at 4 °C.

Analytical Ultracentrifugation. Using fluorophore-labeled DNA and both the sedimentation equilibrium and velocity methods, we have been able to characterize SgrAI−DNA complexes formed with secondary site DNA and precleaved 40 bp primary site containing DNA (Figures 6 and 7). Figure 6A shows the data from sedimentation equilibrium of 7 μM SgrAI and 3.6 μM fluorophore-labeled 18 bp secondary site-containing DNA (HEX-18-2) in binding buffer without glycerol [20 mM Tris-OAc, 50 mM KOAc, 10 mM $Ca(OAc)_2$, and 1 mM DTT] at 4 °C. The binding buffer contains Ca^{2+} which inhibits DNA cleavage by SgrAI. A global fit to a single species using data from two speeds (13500 and 18000 rpm) and two concentrations of SgrAI and DNA (7.0 μM SgrAI and 3.6 μM DNA and 5.4 μM SgrAI and 2.7 μM DNA) resulted in a molecular mass of 90.7 kDa, very close to the calculated molecular mass of the DNA-bound SgrAI dimer (DBD, 87.5 kDa). Hence, SgrAI forms only DBD with this secondary site DNA. The excess SgrAI was added in these experiments to ensure complete binding of the fluorophore-labeled

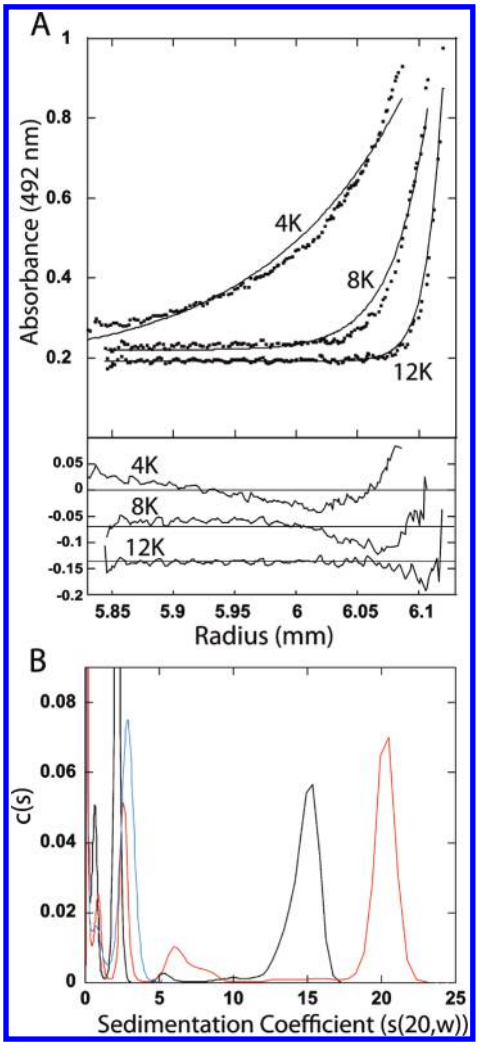

FIGURE 7: Analytical ultracentrifugation of SgrAI with precleaved 40 bp primary site-containing DNA (FLO-PCP). (A) Sedimentation equilibrium experiment with 3 μM SgrAI and 1.5 μM FLO-PCP in 20 mM Tris-OAc (pH 8.0), 50 mM KOAc, 1 mM DTT, and 10 mM $Mg(OAc)_2$ at 37 °C and 4000, 8000, and 12000 rpm. In the top panel, data are shown as filled circles and the line corresponds to a global fit of a single species with a molecular mass of 732 kDa. The bottom panel shows residuals between the fit and data. Residuals in the lower part of panel A were offset for clarity by −0.07 (8K is offset by −0.07 and 12K is offset by −0.14.) (B) Sedimentation velocity experiments with 3 μM FLO-PCP only [blue line, $c(s)$ values scaled by a factor of 0.5] or with 6 μM SgrAI (red and black lines) at 37 °C in 20 mM Tris-OAc (pH 8.0), 1 mM DTT, 10 mM $Mg(OAc)_2$, and either 50 mM KOAc (red and blue lines) or 150 mM NaCl (black line).

DNA, yet the fitted molecular mass from the data indicates that additional SgrAI dimers did not bind to the DNA-bound SgrAI dimer (DBD). Figure 6B shows the $c(s)$ distribution from the sedimentation velocity experiment performed in the same buffer and at the same temperature as the sedimentation equilibrium experiment shown in Figure 6A, with either HEX-18-2 alone (3 μM) (Figure 6B, dotted line) or SgrAI (6 μM) (Figure 6B, solid line). The DNA alone has an s value of 2.2 S, while that in the presence of SgrAI occurs at 5.2 S. Because the sedimentation equilibrium data indicate that the SgrAI−HEX-18-2 complex is predominantly in the form of the DNA-bound SgrAI dimer (DBD), the 5.2 S peak must correspond to the DBD.

Figure 7A shows the result of sedimentation equilibrium experiments performed at three different speeds with 3 μM SgrAI and 1.5 μM fluorophore-labeled precleaved 40 bp primary site-containing DNA (FLO-PCP) in the buffer used for the DNA cleavage assays [20 mM Tris-OAc, 50 mM KOAc, 10 mM $Mg(OAc)_2$, and 1 mM DTT] and at 37 °C. Data were also collected at two other concentrations of SgrAI (6 and 12 μM) and DNA (3 and 6 μM), and the same three speeds. Again, excess SgrAI enzyme was included to ensure complete binding of the fluorophore-labeled DNA. The line in Figure 7A (top panel) corresponds to a fit for a single species of approximately 732 kDa, derived from global fitting of all of the data. The residuals between the fits and the data are shown in the bottom panel of Figure 7A. Clear trends in the residuals can be seen indicating a poor fit of the single-species model to the data; hence, the SgrAI−FLO-PCP complexes must be heterogeneous. In addition, the raised baseline of the data suggests the presence of significantly smaller species that are not sedimented significantly at these speeds (likely the unbound DNA).

Figure 7B shows the $c(s)$ distribution from the sedimentation velocity measurement of either 3 μM FLO-PCP DNA only (Figure 7B, blue line) or 3 μM FLO-PCP DNA with 6 μM SgrAI (Figure 7B, red line), under the same buffer conditions and at the same temperature as the sedimentation equilibrium experiment depicted in Figure 7A. In addition, the sedimentation of a SgrAI−FLO-PCP mixture in a buffer with a higher ionic strength (150 mM NaCl in place of 50 mM KOAc) (Figure 7B, black line) was also analyzed. The data from the FLO-PCP DNA only sample (Figure 7B, blue line) mark the sedimentation of the free DNA, the peaks with sedimentation coefficients of <4 S. The 5−6 S peaks, more prevalent in the lower-ionic strength buffer (Figure 7B, red line), are similar in sedimentation coefficient to the DNA-bound SgrAI dimer (DBD) seen with secondary site DNA in Figure 6B (5.2 S). A shoulder is found with higher s values adjacent to this peak, which may indicate additional species; however, the predominant SgrAI-bound DNA species runs with s values of either 15 or 20 S, depending on the ionic strength of the buffer. The s value of this species is consistent with the high molecular masses derived from the sedimentation equilibrium measurements, and therefore corresponding to the HMWS.

Single-Turnover DNA Cleavage Assays. Single-turnover DNA cleavage rate constants were measured by mixing solutions of ^{32}P-labeled DNA (1 nM) with a solution of enzyme (typically 1 μM) at 37 °C, in buffer supporting DNA cleavage containing 10 mM Mg^{2+} [20 mM Tris-OAc, 50 mM KOAc, 10 mM $Mg(OAc)_2$, and 1 mM DTT]. Some reactions were also performed at 4 °C. The amount of DNA cleaved with time was measured by quenching aliquots of the reaction mixtures at different times after mixing the SgrAI enzyme with the DNA, separating cleaved from uncleaved DNA via denaturing PAGE, and quantitating by autoradiography. The amount of cleaved DNA was normalized (using either the total intensity of the lane or the sum of the amount of cleaved and uncleaved DNA in the same lane) and then plotted versus time. Unlabeled DNA was added in some reactions to test for its stimulatory capacity and was added to the solution with the labeled DNA prior to being mixed with the enzyme solution. The resulting single-turnover rate constants measured for DNA cleavage of various sequences by SgrAI are presented in Table 2. Most data fit well ($R > 0.99$) to a single-exponential equation (see Experimental Procedures), while the data with 0.9 μM 40 bp uncleaved primary site DNA (40-1) (Table 2) required two exponential functions to fit the data. The total amount of labeled DNA that was cleaved in each reaction varied, in some cases because of the melting of the duplex into single strands (which cannot be cleaved by SgrAI) as a consequence of repeated freezing and thawing of the labeled DNA stock solution. However, the amount of secondary site DNA cleaved did show a systematic trend in which a larger fraction was cleaved with increasing amounts of added unlabeled precleaved 40 bp primary site-containing DNA (PCP). The percent of the DNA cleaved was then very carefully measured in triplicate, in single-turnover reactions performed simultaneously.

Table 2: Single-Turnover DNA Cleavage Rate Constants Using 1 μM SgrAI at 37 °C (unless otherwise noted)

^{32}P-labeled DNA (1 nM)	concn of added unlabeled DNA	WT SgrAI rate constant (min^{-1})
primary site (18-1, 18 bp)	none	0.094 ± 0.015
	10 nM PCP	0.18 ± 0.06
	100 nM PCP	0.30 ± 0.03
	1 μM PCP	>20
	1 μM PCP (QF)[a]	22 ± 7
	2 μM PCP	>20
	0.9 μM 18-1	0.063 ± 0.006
	0.9 μM 40-1	10.0 ± 1.4 (56 ± 2%)
		0.032 ± 0.012 (44 ± 2%)
	0.9 μM 40-2	0.16 ± 0.06
	none, 4 °C	$<4 \times 10^{-5}$[b]
	0.9 μM 18-1, 4 °C	0.118 ± 0.014
	0.9 μM PC, 4 °C	2.2 ± 0.04
primary site (40-1, 40 bp)	none	0.14 ± 0.05
	0.9 μM 40-1	>20 (22 ± 9%)
		0.024 ± 0.008 (78 ± 9%)
secondary site (18-2, 18 bp)	none	0.020 ± 0.006 (2.8 ± 0.6%)
	10 nM PCP	0.012 ± 0.001[c] (3.4 ± 0.1%)[c]
	100 nM PCP	0.016 ± 0.005 (19 ± 5%)
	1 μM PCP	0.05 ± 0.01 (24 ± 1%)

[a]QF indicates the measurement was taken in the Kintek RQF-3 rapid quench flow instrument. [b]No cutting detected after incubation for 21 h. Rate constant estimated assuming 5% cleavage or less after 21 h. [c]Only two repetitions.

The rate constants for cleavage of primary site DNA embedded in constructs with different amounts of flanking DNA, 18-1 and 40-1, are very similar: 0.094 ± 0.015 and 0.14 ± 0.05 min^{-1}, respectively. The rate constant for cleavage of secondary site DNA (18-2), in the absence of added precleaved 40 bp primary site-containing DNA (PCP), was only ~5-fold smaller than that for primary site DNA (18-1) (0.020 ± 0.006 min^{-1}). Added PCP increased the rate constant for cleavage of 1 nM ^{32}P-labeled primary site DNA (18-1) dramatically, from 0.094 to >20 min^{-1} with 1 μM PCP, a rate too fast to measure

by hand. Using a quench flow instrument, this rate constant was measured as 22 ± 7 min^{-1}, representing a >200-fold increase. Similarly, added 40-1 (0.9 μM) also stimulated cleavage of 1 nM ^{32}P-labeled primary site DNA (18-1 or 40-1), to a rate too fast to measure by hand (> 20 min^{-1}), although only a portion of the total amount of cleaved DNA was cleaved with an accelerated rate. In contrast, added unlabeled 18-1 (0.9 μM) did not stimulate primary site DNA cleavage by SgrAI (at 37 °C), and neither did unlabeled 0.9 μM 40-2 (0.16 ± 0.06 min^{-1}), the secondary site embedded in the same oligonucleotide as 40-1.

The cleavage of secondary site DNA (18-2) was also stimulated by added precleaved 40 bp primary site-containing DNA (PCP), from 0.020 ± 0.006 min^{-1} in the absence of PCP to 0.05 ± 0.01 min^{-1} in the presence of 1 μM PCP, an increase of a factor of ~2.5. More significantly, the percentage of secondary site DNA cleaved by SgrAI was very low in the absence of PCP and is increased from ~2 to ~24% with 1 μM PCP. The total amount of DNA cleaved reaches a maximum at ~25% cleavage rather than 100%, most likely because of the dissociation of duplex DNA into single strands during freezing for storage of the DNA.

Cleavage reactions were also performed at 4 °C with 1 nM ^{32}P-labeled 18 bp primary site DNA (18-1) and 1 μM SgrAI, with or without 0.9 μM unlabeled DNA, either 18-1 or precleaved 40 bp primary site DNA (PC, as in PCP without the 5′-phosphate at the cleavage site). No cleavage of the labeled DNA was detected in the absence of the additional DNA, even after 21 h, suggesting a rate constant of $< 4 \times 10^{-5}$ min^{-1} (assuming a 5% cleavage limit of detection). However, the presence of 0.9 μM 18-1 stimulates cleavage, with a rate constant of 0.118 ± 0.014 min^{-1}. Therefore, although 18-1 fails to stimulate DNA cleavage at 37 °C, stimulation of DNA cleavage by 18-1 does occur at 4 °C. The cleavage of 1 nM 18-1 at 4 °C is also stimulated by PC to 2.2 ± 0.04 min^{-1}, indicating that the stimulatory capacity of 18-1 is smaller than that of PC DNA.

DISCUSSION

DNA binding and stoichiometric measurements indicated very tight binding (nanomolar or better) to the primary and secondary site DNA constructs used in this study, with 1:1 binding of the SgrAI dimer to the 18 bp duplex DNA (Table 1 and Results).

In addition, a method developed for the separation of different DNA-bound forms of SgrAI using native gel electrophoresis showed the presence of two DNA-bound SgrAI forms (Figures 3 and 4). The faster-moving species is identified as the DNA-bound SgrAI dimer (DBD), because sedimentation measurements (see below) show that only DBDs are formed with the secondary site DNA 18-2, and only this band is seen with 18-2 (Figure 3, lanes 7−9). The slower-moving species, which barely enters the gel, has been termed HMWS, as it has been determined to be quite large by analytical ultracentrifugation (Figure 7). The HMWS forms only under certain conditions, namely, a case in which sufficient concentrations of both SgrAI and primary site DNA (cleaved or uncleaved) are present. DNA containing only the secondary site, whether in an 18 or 40 bp duplex (i.e., 18-2 or 40-2, respectively), will not form HMWS without the presence of any primary site (Figure 3). Secondary site DNA bound to SgrAI can, however, become part of the HMWS in the presence of primary site DNA (Figures 3 and 4). Precleaved 40 bp primary site-containing DNA (PCP) also stimulates formation of HMWS. Comparison of the ability of uncleaved primary site-containing DNA (with different lengths of flanking DNA, 18-1 or 40-1) and PCP to induce formation of HMWS with ^{32}P-labeled 18-1 shows similar activities (Figure 4C). Analysis of the concentration dependence of HMWS formation shows a midpoint to saturation at ~100 nM DNA, which corresponds to ~100 nM DBD, because at 1 μM SgrAI nearly all DNA will be bound. These results also explain why no cooperativity was seen in the FPA and gel shift assays used to measure DNA binding affinity, because at 1 nM DNA, the concentration of the DBD would be too low to form HMWS.

Analytical ultracentrifugation was used to analyze the size of the HMWS. Fluorophore-labeled DNA was used to limit detection to only DNA-containing species. However, unlike the native gel electrophoresis described above, the higher concentrations of DNA necessary for detection, 2.7−3.6 μM DNA (and 5.4−7.0 μM SgrAI), were used in this study. Figure 7A shows the data from a sedimentation equilibrium experiment with 1.5 μM fluorophore-labeled precleaved 40 bp primary site-containing DNA (FLO-PCP) and 3 μM SgrAI, in the same buffer used for the DNA cleavage assays at 37 °C. Data from Figure 7A, as well as at two higher concentrations of SgrAI and DNA, were globally fit to an equation for a single species, resulting in a fitted molecular mass of 723 kDa. Clearly, the data do not fit well to this single-species model, indicating heterogeneity (Figure 7A). Fits to individual sedimentation equilibrium curves led to estimates of molecular masses ranging from 400 to 1200 kDa. Hence, the species formed by SgrAI and FLO-PCP are large and heterogeneous, with DBDs associating in numbers in the range of 4−12 (the calculated molecular mass of the SgrAI dimer bound to two molecules of FLO-PCP is approximately 101.5 kDa). The large size is consistent with the native PAGE that indicated it to be a species larger than the DNA-bound SgrAI dimer (DBD). A large, heterogeneous species was also detected in a previous report (*4*), using SgrAI and a 20 bp primary site-containing DNA, with a rough estimate of ~7 DBDs reported (*4*). The previous study utilized a buffer containing Ca^{2+}, rather than Mg^{2+}, and the experiments were performed at 4 °C rather than 37 °C (*4*). Therefore, the formation and size of the HMWS appear to be relatively independent of the temperature, the type of divalent cation (Ca^{2+} or Mg^{2+}), the length of the DNA flanking the primary site sequence, and whether the site is cleaved.

In contrast to the results with FLO-PCP, the sedimentation equilibrium experiment with secondary site-containing DNA (HEX-18-2) indicates that only DBDs are present (the fit provides a molecular mass of 90.7 kD, while the predicted DBD molecular mass is 87.5 kDa) (Figure 6A). Sedimentation distributions with only HEX-18-2 DNA (3 μM) (Figure 6B, dotted line) or with HEX-18-2 and SgrAI (3 and 6 μM, respectively) (Figure 6B, solid line), under identical buffer conditions and at identical temperatures, show free DNA having a sedimentation coefficient of 2.2 S, and 5.2 S for the SgrAI−DNA complex. Because the sedimentation equilibrium experiment indicates that the SgrAI-bound DNA is predominantly in the form of DBD (Figure 6A), the single SgrAI-bound DNA peak in the $c(s)$ distribution at 5.2 S (Figure 6B, solid line) must correspond to the DBD.

The $c(s)$ distribution from the sedimentation velocity experiment with SgrAI (6 μM) and precleaved 40 bp primary site-containing DNA (FLO-PCP) (3 μM) shows several species (Figure 7B). In this case, the buffer conditions and temperature are those used in the DNA cleavage measurements (Figure 7B, red line) or in a buffer with a higher ionic strength (150 mM NaCl in place of the 50 mM KOAc of the DNA cleavage buffer) (Figure 7B, black line). The two peaks with the smallest s values

correspond to free DNA (Figure 7B, blue line). A peak appears at 5−6 S, similar in size to the DBD formed by SgrAI and HEX-18-2 (5.2 S). The majority of the SgrAI-bound DNA is found sedimenting with coefficients of 15 and 20 S. The sedimentation coefficients differ depending on the ionic strength of the buffer, perhaps because of dissociation (*22*), effects on size, shape, or solvation, or the variation from sample to sample in fitting multipeak data.

The excess SgrAI (over DNA) concentration used in the sedimentation experiments with FLO-PCP could result in additional SgrAI dimers binding to the SgrAI−FLO-PCP complex. However, the species with high sedimentation coefficients found in this study (20 S in the buffer with 150 mM NaCl) is similar in sedimentation coefficient (20 S) to that described in the previous study (*4*) that used a 1:1 molar ratio of SgrAI to DNA in a buffer with 150 mM KOAc, and a DNA with very short flanking sequences (a 20 bp uncleaved primary site-containing DNA). The additional excess SgrAI enzyme was also used in the sedimentation experiments with HEX-18-2 yet did not lead to additional SgrAI dimers binding to the SgrAI−DNA complex. Native gels do indicate that additional SgrAI dimers bind to the SgrAI−PCP complex (Figure 3, lane 13); however, these complexes are distinct from the HMWS in that they migrated separately and faster, indicating that they were smaller than the HMWS. This faster-migrating species occurred only with lower concentrations of the DNA-bound SgrAI dimer (DBD), and once the concentration of the DBD increased above ~100 nM, only HMWS were observed. The native PAGE results argue that the HMWS is composed of oligomers of DBD, because the formation of HMWS is dependent on the concentration of DBD and not merely SgrAI dimer concentration; however, they do not rule out the binding of additional SgrAI dimers to the oligomerized SgrAI−PCP complex. Thus, the estimated size of the HMWS formed by SgrAI and PCP, under buffer conditions supporting DNA cleavage (and at 37 °C, where the DNA cleavage measurements have been taken), of 4−12 DBDs may include the presence of additional SgrAI dimers with the oligomerized DBD. In any event, the DNA cleavage measurements also typically have an excess of SgrAI dimer over DNA, and therefore, this measurement of the size of the HMWS may actually be more relevant than a measurement with an alternative ratio of SgrAI to DNA.

The single-turnover rate constants for DNA cleavage of the primary site in the two different length duplexes (18-1 and 40-1) and with a secondary site DNA (18-2) were measured (Table 2). The reactions were performed at 37 °C (unless otherwise specified) with 10 mM Mg^{2+} (rather than Ca^{2+}) and in the absence of glycerol, but the buffer components were otherwise the same as those for the FPA and native PAGE. The concentration of SgrAI in the measurements was 1 μM, to ensure complete saturation of the ^{32}P-labeled DNA, which was 1 nM at the initiation of the reactions. The rate constants for cleavage of the primary site DNAs were found to be similar, 0.094 ± 0.015 and 0.14 ± 0.05 min^{-1} for 18-1 and 40-1, respectively, indicating that the added flanking DNA of 40-1 does not greatly influence the DNA cleavage rate constant. These numbers compare well to a previously published single-turnover cleavage rate constant on plasmids with single primary sites (*4*), 0.04 min^{-1}. The rate constant for cleavage of the secondary site, 18-2, was measured to be 0.020 ± 0.006 min^{-1} (Table 2), only 5-fold slower than that of the primary site in the same length DNA. This rate constant is similar to that found using steady state kinetics for a secondary site in an 80 bp duplex (*8*), 0.012 min^{-1}. Cleavage of both primary and secondary site DNA was found to be stimulated under the conditions of the assay, by the addition of primary site DNA (40-1, PCP) with sufficient flanking sequences. Both 40-1 and PCP (precleaved 40 bp primary site-containing DNA) stimulated cleavage of 18-1 by 1 μM SgrAI to a rate constant of > 20 min^{-1}, too fast to measure by hand. The rate constant was measured by quench flow as 22 ± 7 min^{-1} (with 1 μM PCP), a stimulatory factor of > 200-fold. Stimulation of cleavage of 20 and 30 bp oligonucleotides with primary and secondary sites has been observed previously, using a 30 bp oligonucleotide with a primary site sequence, although rate constants were not reported (*7*). Surprisingly, the 18-1 DNA could not stimulate its own cleavage (at 37 °C), even at 0.9 μM (and 1 μM SgrAI), similar to that reported using a 20 bp primary site duplex (*4*). The requirement for sufficient flanking DNA to provide stimulation was seen in a previous study (*7*), as well as the ability of both the uncleaved and cleaved primary site to stimulate DNA cleavage by SgrAI (*5*, *7*, *8*). Flanking DNA itself however is not sufficient as a construct with the same flanking DNA, but a secondary site (40-2), rather than a primary site, did not stimulate DNA cleavage (at a concentration of 0.9 μM with 1 μM SgrAI) (Table 2). Previous measurements of DNA cleavage under stimulated conditions at 37 °C include a single-turnover DNA cleavage rate constant measured with a plasmid containing two recognition sites (*4*) (0.5−0.7 min^{-1}) and with an 80 bp duplex using steady state kinetics (*8*) (2.4 min^{-1}), and the same duplex but added precleaved primary site-containing DNA (16.2 min^{-1}) (using steady state kinetics). Our measurement of the maximally stimulated primary site DNA cleavage by SgrAI compares best to the latter example.

The stimulation of primary site DNA cleavage increased with an increasing concentration of added precleaved 40 bp primary site-containing DNA (PCP) by at least 200-fold; however, the level of stimulation of secondary site DNA increased by only ~2.5-fold, to 0.05 ± 0.01 min^{-1}. This value is similar to that found by Wood et al. (*7*), in the single-turnover cleavage of secondary sites on plasmid DNA with primary sites (0.08 min^{-1}). However, more significantly, the overall percent of secondary site DNA that was cleaved by the end of the reaction was much greater with higher concentrations of PCP. The total amount of DNA cleaved appears to reach a maximum at only 24%, probably because a majority of it is single-stranded after repeated freezing and thawing of the labeled DNA. In the absence of PCP, only 2%, or 10% of the final fully cleavable amount, is cleaved by SgrAI. The stimulated rate constant for cleavage of the secondary site we measure (0.05 ± 0.01 min^{-1}) is 5 times slower than that measured using steady state kinetics with an 80 bp duplex (0.35 min^{-1}) (*8*); however, a different secondary site sequence was used in our study (CACCGGGG compared to CACCGGCT).

The effects of buffer conditions such as ionic strength, temperature, and divalent cation cofactor were tested on formation of the HMWS using either the native gel electrophoresis analysis or the sedimentation velocity method. First, the formation of HMWS at 4 °C analyzed using the native gel electrophoresis assay with samples incubated in buffers containing 10 mM Ca^{2+} and either 0−300 mM KOAc or 0−300 mM NaCl (Figure 5) showed that HMWS formed with radiolabeled 18 bp DNA containing the primary site sequence (18-1), and precleaved 40 bp primary site-containing DNA (PC) was stable at all ionic strengths tested. Hence, the HMWS is not an artifact of a low ionic strength. Sedimentation velocity experiments conducted at 37 °C with 10 mM Mg^{2+}, 6 μM SgrAI, and 3 μM fluorophore-labeled precleaved 40 bp primary site-containing DNA (FLO-PCP) in buffer containing either 50 mM KOAc or 150 mM NaCl

(Figure 7B) show changes in the centering of the peak designated as HMWS, indicating altered sedimentation coefficients; again, the higher ionic strength does not eliminate the presence of the HMWS. In addition, the fact that HMWS was detected in the sedimentation experiments performed with Mg^{2+} at 37 °C (Figure 7) shows that the HMWS is not an artifact of the Ca^{2+} or temperature (4 °C) used in the native gel electrophoresis assays.

In a previous study, steady state kinetic measurements of the cleavage of 80 bp DNA constructs containing primary or secondary site DNA showed Hill coefficients of 2−4 (*8*). These Hill coefficients are reduced to ~1 when an added precleaved primary site DNA is added, supporting the cooperativity of DNA concentration in enhancing DNA cleavage. The cooperativity seen with secondary site DNA, in the absence of any primary site DNA, may appear contradictory to the results presented here that show no DNA cleavage stimulation in single-turnover cleavage assays by the addition of secondary site DNA. However, upon cleavage of secondary site DNA, two cleaved ends are produced, one of which is exactly the same as a cleaved primary site. With multiple enzyme turnovers, as in the steady state kinetic assay, these species can accumulate to sufficient concentrations to influence the reaction kinetics. Therefore, the cooperativity seen in the steady state kinetics with secondary site DNA and the lack of stimulation by secondary site DNA seen in this work are consistent if the species mediating the cooperativity in the steady state kinetics is the product of secondary site DNA cleavage.

The self-activation of DNA cleavage by SgrAI implies allostery, where at a minimum low- and high-activity conformations exist in an equilibrium that can be shifted by the interaction with an allosteric effector. The fact that the addition of precleaved 40 bp primary site-containing DNA (PCP) can enhance the DNA cleavage rate by SgrAI suggests the existence of more than one DNA binding site on the functional SgrAI molecule. Type II restriction endonucleases typically bind to duplex DNA as dimers, in a 1:1 complex; however, several type II restriction endonucleases form tetramers in solution and bind to two DNA duplexes. SgrAI shares amino acid sequence similarity and DNA cleavage sequence similarity with three such enzymes: NgoMIV, Cfr10I, and Bse634I. Therefore, it was reasonable to consider that SgrAI might also form a tetramer with two DNA binding sites under activating conditions. Analytical ultracentrifugation of the SgrAI enzyme showed it to exist as a dimer in solution in the absence of DNA (*4*); with DNA, it formed a 1:1 complex of SgrAI dimer to DNA duplex that appeared to aggregate into a very large species, large enough to accommodate at least seven SgrAI dimers bound to duplex DNA (*4*). Still, the model for SgrAI activity included slow cleavage of DNA by SgrAI dimers, and association of dimers bound to cleaved DNA with other dimers bound to uncleaved DNA to form an activated tetramer (*4*, *7*, *8*). The activated tetramer conformation is predicted by the model to exhibit very fast cleavage of DNA. In addition, the activated DNA-bound dimers could dissociate from the tetramer and associate with other DNA-bound dimers, thus activating them; hence, a chain reaction would result in the overall observed accelerated DNA cleavage rate. The addition of precleaved primary site DNA presumably accelerated the rate of DNA cleavage by inducing the activated conformation and stimulating dimers to form tetramers with the activated conformation. Structural studies reported to date show a dimer of SgrAI bound to a single duplex of primary site-containing DNA (the 18-1 construct used in this study), which is considered to be in a low-activity conformation (*9*). A structure of the activated conformation has not yet been reported, and no direct data that support a tetrameric form of SgrAI as the activated species exist.

Native PAGE and analytical ultracentrifugation were successful in unambiguously demonstrating the presence of DNA-bound species of SgrAI larger than dimers (Figures 3−5 and 7). Identified as HMWS on native gels, the sedimentation measurements indicate that HMWS composed of SgrAI and PCP is heterogeneous containing possibly as many as 4−12 DNA-bound SgrAI dimers (DBD). We found that formation of the HMWS species by SgrAI is dependent on DNA sequence (requiring the primary site sequence) and dependent on the concentration of DNA-bound SgrAI dimer (DBD) (forming significantly with ≥100 nM DBD in our assays), and HMWS can form with either cleaved or uncleaved primary site-containing DNA. We also found that HMWS formation did not depend on the divalent cation or temperature used in the assays, as HMWS is observed in assays with either Ca^{2+} or Mg^{2+}, and at both 4 and 37 °C. Initially, we used the precleaved primary site (PCP) DNA to induce HMWS and to stimulate DNA cleavage, although we later determined that uncleaved 40 bp primary site-containing DNA (40-1) can also induce HMWS. We found that added PCP stimulated both HMWS formation (in 10 mM Ca^{2+} or Mg^{2+} at 4 °C) and DNA cleavage (10 mM Mg^{2+} at 37 °C) with 1 nM uncleaved (primary or secondary site) DNA at similar concentrations of PCP (100−1000 nM). Because both DNA cleavage activity and the oligomerization of DBD into HMWS are dependent on the concentrations of added PCP, we propose that the HMWS is the activated (or activatable) form of the enzyme. Activation by oligomerization is a very unusual mechanism, although it has been proposed in one other system, that of acetyl-CoA carboxylase (*23*).

The simplest model of DNA cleavage by SgrAI includes two conformations of SgrAI, a low-activity form and a high-activity form. In such a model, intermediate rate constants for DNA cleavage should not occur, because there are no conformations with intermediate levels of activation. Instead, in cases where only a subset of the total population of enzymes is stimulated, the amount of cleaved DNA with time would be the sum of that from two independent first-order processes from the two enzyme states, and therefore, the data for cleaved DNA with time should fit to two-exponential functions. This was true in the assays with 0.9 μM 40 bp primary site-containing DNA (40-1), where a portion of the labeled DNA was cleaved at a much stimulated rate, and a portion was cleaved at the lower, unstimulated rate. However, the experimental data using precleaved 40 bp primary site-containing DNA (PCP) as the stimulating DNA are best fit not with multiple-exponential functions, but rather only a single-exponential function. The measured rate constants increase with the concentration of added PCP, such that with intermediate concentrations of PCP, intermediate values of the rate constant are exhibited (Table 2). If the rate constants measure the actual rate of the chemical step in DNA cleavage, they then indicate that intermediate levels of enzyme activation exist. However, because these first-order rate constants vary with the concentration of added PCP, they could also be pseudo-first-order rate constants for a second-order process that is dependent on PCP concentration, which occurs prior to DNA cleavage, for example, the binding of DNA to SgrAI, or the association of the SgrAI dimer bound to ^{32}P-labeled 18 bp primary site-containing DNA (18-1) with SgrAI dimers bound to PCP. The association of DNA binding proteins with DNA is typically very fast (*24*); therefore, the association of the DNA-bound dimers could be the

second-order process that governs the observed kinetics. In the case of the cleavage of the secondary site DNA, the observed kinetics appear more like the contributions from two enzyme states, one that is completely inactive and another that has a maximal rate of cleavage that is similar to the slow cleavage rate of primary site DNA. Roughly the same cleavage rate constant is measured in the absence and presence of stimulation, but a greater percentage of the secondary site DNA is cleaved under stimulatory conditions. Therefore, the apparent alteration of sequence specificity in SgrAI appears to involve the switching on of DNA cleavage at a sequence already bound tightly by the enzyme, through shifting the enzyme conformation to a more active form. However, the cleavage rate on secondary site DNA is never stimulated to nearly the same extent as that on primary site DNA, suggesting that the secondary site sequence may impede the attainment of the fully activated conformation by SgrAI or the SgrAI−DNA complex.

We found that uncleaved primary site DNA, if present in a 40 bp duplex (40-1), is capable of stimulating both formation of high-molecular weight species (HMWS) (using native PAGE) and DNA cleavage (in single-turnover assays). However, 40-1 when cleaved creates two molecules of PCP, which also have stimulatory properties, and we wonder if it is the PCP that induces the activated conformation, and HMWS is a form required for the activated conformation but is actually capable of both low- and high-activity conformations. However, the rate of unstimulated cleavage of 40-1 is 0.14 ± 0.05 min^{-1}, while the activated cleavage rate is >20 min^{-1}, too fast for significant amounts of PCP to be created by DNA cleavage. Therefore, it may be that the HMWS is the activated conformation itself, which is capable of forming with Ca^{2+}, and forms with sufficient concentrations of DNA-bound SgrAI dimer regardless of the presence or absence of cleavage, explaining the ability of 40-1 to both induce HMWS and stimulate prior to its own cleavage. Alternatively, within the HMWS, a small amount of cleavage of 40-1 into PCP could be rapidly communicated, and cleavage of all DNA in the HMWS then rapidly performed. If true, the HMWS would be capable of both the low- and high-activity conformations, cleaved DNA would be the signal to shift conformation, and the communication of DNA cleavage in one dimer would induce the conformational change in all associated SgrAI enzymes in the HMWS. Further studies with uncleavable substrates could address this question.

In contrast to the results with the 40 bp primary site-containing DNA (40-1) and the precleaved 40 bp primary site-containing DNA (PCP or PC), the primary site in an 18 bp duplex (18-1) does not stimulate DNA cleavage under single-turnover cleavage assay conditions (i.e., 37 °C and 10 mM Mg^{2+}) but does stimulate formation of HMWS under binding assay conditions (i.e., 4 °C and 10 mM Ca^{2+}). The lack of correlation of HMWS formation and stimulatory capacity with 18-1 could be due to the different conditions of the two assays; for example, the lower temperature and/or Ca^{2+} may stabilize HMWS that is not stable at 37 °C with Mg^{2+}. Our binding affinity measurements of SgrAI with DNA suggested a 5-fold lower K_D in the presence of Ca^{2+} relative to Mg^{2+}. If the lack of stimulatory activity by 18-1 is due to diminished HMWS stability, then the role of the flanking DNA in stabilizing HMWS suggests perhaps an additional albeit non-sequence specific DNA binding site on SgrAI. To investigate this issue further, we performed single-turnover DNA cleavage assays at 4 °C. No cleavage of 1 nM ^{32}P-labeled 18-1 by 1 μM SgrAI was found, even after incubation for 21 h. However, with 0.9 μM unlabeled 18-1 added to the reaction mixture, the labeled DNA was found to be cleaved with a rate constant of 0.118 ± 0.014 min^{-1}. PC DNA was found to stimulate the cleavage more effectively, with a measured rate constant of 2.2 ± 0.04 min^{-1}. The failure of 18-1 to stimulate cleavage at 37 °C, but successfully at 4 °C, is consistent with the proposal that the lower temperature stabilizes HMWS. The stabilization may occur through altered thermodynamic properties of the complex, or alternatively through prevention of dissociation of cleaved 18-1 into single strands, if cleaved DNA is the signal for activation. The cleavage rate constants obtained with 40-1 (see above) argue against cleaved DNA as the activation signal unless the signal is propagated within the HMWS. We did find that SgrAI behaved differently with precleaved primary site-containing DNA compared to 40-1, its uncleaved version, in the formation of HMWS and in the cleavage assays; while PCP stimulated accelerated cleavage of all of the labeled DNA in the assays, 40-1 stimulated the cleavage of only a portion. However, recent structural studies of SgrAI bound to cleaved primary site DNA argue against the cleaved primary site itself as the stimulatory signal (*25*); this structure contains the 18 bp primary site DNA, and the SgrAI−DNA complex is in the DNA-bound dimer form. Structural characterization of the HMWS will be key to understanding the origin of the activation signal.

The unusual DNA cleavage activity of SgrAI may be a consequence of the large genome of *S. griseus,* from which it is derived. Restriction endonucleases are coexpressed with a methyltransferase enzyme having the same sequence specificity, which functions to protect the host genome from the cleavage activity of the endonuclease. Hence, the SgrAI methyltransferase must methylate all SgrAI recognition sequences within the genome before cleavage by the endonuclease can occur, and this requirement may be difficult because of the large size of the genome (>8 million bp). The relatively long sequence recognized by SgrAI, 8 bp versus the usual 4−6 bp, may have evolved because of this pressure, because the longer sequence greatly reduces the number of sites to be methylated in the host DNA. In addition, the inherently low cleavage activity of SgrAI in the absence of cleaved primary site DNA also reduces the pressure on host DNA, as well as the methyltransferase enzyme. However, such a long recognition sequence will also occur far less frequently in the phage DNA and hence place selective pressure on the enzyme for increased activity for adequate protection of the host from phage infection. It appears that one way in which the SgrAI enzyme activity is increased is through the stimulation of its cleavage activity. Another way is through its secondary site cleavage activity, which will induce more cleavages in the phage DNA than at the primary sites alone and hence could better protect the host. These secondary sites of the host are normally protected from SgrAI cleavage activity, because cleavable primary sites are required to induce secondary site cleavage, and primary sites are protected by methylation in the host. However, activation of SgrAI by invading phage could result in cleavage of the host DNA, in addition to phage DNA, at the secondary sites. Therefore, the formation of aggregates, or oligomers, of DNA-bound dimers may have an important role in sequestering activated SgrAI on the phage DNA and away from the host genomic DNA.

ACKNOWLEDGMENT

We acknowledge the Analytical Biophysics Core Facility at the University of Arizona for the analytical ultracentrifugation data and its interpretation.

REFERENCES

1. Pingoud, A., Fuxreiter, M., Pingoud, V., and Wende, W. (2005) Type II restriction endonucleases: Structure and function. *Cell. Mol. Life Sci. 62*, 685–707.
2. Tautz, N., Kaluza, K., Frey, B., Jarsch, M., Schmitz, G. G., and Kessler, C. (1990) SgrAI, a novel class-II restriction endonuclease from *Streptomyces griseus* recognizing the octanucleotide sequence 5′-CR/CCGGYG-3′ [corrected]. *Nucleic Acids Res. 18* (10), 3087.
3. Bilcock, D. T., Daniels, L. E., Bath, A. J., and Halford, S. E. (1999) Reactions of type II restriction endonucleases with 8-base pair recognition sites. *J. Biol. Chem. 274* (51), 36379–36386.
4. Daniels, L. E., Wood, K. M., Scott, D. J., and Halford, S. E. (2003) Subunit assembly for DNA cleavage by restriction endonuclease SgrAI. *J. Mol. Biol. 327* (3), 579–591.
5. Bitinaite, J., and Schildkraut, I. (2002) Self-generated DNA termini relax the specificity of SgrAI restriction endonuclease. *Proc. Natl. Acad. Sci. U.S.A. 99* (3), 1164–1169.
6. Pingoud, A., and Jeltsch, A. (2001) Structure and function of type II restriction endonucleases. *Nucleic Acids Res. 29* (18), 3705–3727.
7. Wood, K. M., Daniels, L. E., and Halford, S. E. (2005) Long-range communications between DNA sites by the dimeric restriction endonuclease SgrAI. *J. Mol. Biol. 350* (2), 240–253.
8. Hingorani-Varma, K., and Bitinaite, J. (2003) Kinetic analysis of the coordinated interaction of SgrAI restriction endonuclease with different DNA targets. *J. Biol. Chem. 278* (41), 40392–40399.
9. Dunten, P. W., Little, E. J., Gregory, M. T., Manohar, V. M., Dalton, M., Hough, D., Bitinaite, J., and Horton, N. C. (2008) The structure of SgrAI bound to DNA; recognition of an 8 base pair target. *Nucleic Acids Res. 36*, 5405–5416.
10. Aggarwal, A. K. (1990) Crystallization of DNA binding proteins with oligodeoxynucleotides. *Methods: A Companion to Methods in Enzymology 1*, 83–90.
11. Fasman, G. D. (1975) CRC Handbook of Biochemistry and Molecular Biology, 3rd ed., CRC, Cleveland, OH.
12. Reid, S. L., Parry, D., Liu, H. H., and Connolly, B. A. (2001) Binding and recognition of GATATC target sequences by the EcoRV restriction endonuclease: A study using fluorescent oligonucleotides and fluorescence polarization. *Biochemistry 40* (8), 2484–2494.
13. Carey, J. (1991) Gel retardation. *Methods Enzymol. 208*, 103–117.
14. Sambrook, J., Fritsch, E. F., and Maniatis, T. (1989) Molecular cloning: A laboratory manual, 2nd ed., p 3 v, Cold Spring Harbor Laboratory Press, Plainview, NY.
15. Abramoff, M. D. (2009) Image Processing with ImageJ. *Biophotonics Int. 11* (7), 36–42.
16. Schuck, P. (2000) Size-distribution analysis of macromolecules by sedimentation velocity ultracentrifugation and lamm equation modeling. *Biophys. J. 78* (3), 1606–1619.
17. Laue, T. M., Shah, B. D., Ridgeway, T. M., and Pelletier, S. L. (1992) Computer-aided interpretation of analytical sedimentation data for proteins. In Analytical Ultracentrifugation in Biochemistry and Polymer Science (Harding, S. E., Rowe, A. J., and Horton, J. C., Eds.) pp 90−125, Royal Society of Chemistry, Cambridge, U.K.
18. Vipond, I. B., and Halford, S. E. (1995) Specific DNA recognition by EcoRV restriction endonuclease induced by calcium ions. *Biochemistry 34* (4), 1113–1119.
19. Martin, A. M., Horton, N. C., Lusetti, S., Reich, N. O., and Perona, J. J. (1999) Divalent metal dependence of site-specific DNA binding by EcoRV endonuclease. *Biochemistry 38* (26), 8430–8439.
20. Etzkorn, C., and Horton, N. C. (2004) Ca^{2+} binding in the active site of HincII: Implications for the catalytic mechanism. *Biochemistry 43* (42), 13256–13270.
21. Joshi, H. K., Etzkorn, C., Chatwell, L., Bitinaite, J., and Horton, N. C. (2006) Alteration of sequence specificity of the type II restriction endonuclease HincII through an indirect readout mechanism. *J. Biol. Chem. 281* (33), 23852–23869.
22. Schuck, P. (2010) Diffusion of the reaction boundary of rapidly interacting macromolecules in sedimentation velocity. *Biophys. J. 98* (11), 2741–2751.
23. Brownsey, R. W., Boone, A. N., Elliott, J. E., Kulpa, J. E., and Lee, W. M. (2006) Regulation of acetyl-CoA carboxylase. *Biochem. Soc. Trans. 34* (Part 2), 223–227.
24. Halford, S. E. (2009) An end to 40 years of mistakes in DNA-protein association kinetics? *Biochem. Soc. Trans. 37* (Part 2), 343–348.
25. Little, E. J., Dunten, P. W., Bitinaite, J., and Horton, N. C. (2010) Structures of SgrAI Bound to Cleaved Primary Site DNA and Uncleaved Secondary Site DNA. (submitted for publication).